



The World's Largest Open Access Agricultural & Applied Economics Digital Library

This document is discoverable and free to researchers across the globe due to the work of AgEcon Search.

Help ensure our sustainability.

Give to AgEcon Search

AgEcon Search
<http://ageconsearch.umn.edu>
aesearch@umn.edu

Papers downloaded from AgEcon Search may be used for non-commercial purposes and personal study only. No other use, including posting to another Internet site, is permitted without permission from the copyright owner (not AgEcon Search), or as allowed under the provisions of Fair Use, U.S. Copyright Act, Title 17 U.S.C.

No endorsement of AgEcon Search or its fundraising activities by the author(s) of the following work or their employer(s) is intended or implied.



A Monte Carlo Study of Multiplicity Fluctuations in Pb-Pb Collisions at LHC Energies

Ramni Gupta*

Department of Physics & Electronics, University of Jammu, Jammu, India

Abstract

With large volumes of data available from LHC, it has become possible to study the multiplicity distributions for the various possible behaviours of the multiparticle production in collisions of relativistic heavy ion collisions, where a system of dense and hot partons has been created. In this context it is important and interesting as well to check how well the Monte Carlo generators can describe the properties or the behaviour of multiparticle production processes. One such possible behaviour is the self-similarity in the particle production, which can be studied with the intermittency studies and further with chaoticity/erraticity, in the heavy ion collisions. We analyse the behaviour of erraticity index in central Pb-Pb collisions at centre of mass energy of 2.76 TeV per nucleon using the AMPT monte carlo event generator, following the recent proposal by R.C. Hwa and C.B. Yang, concerning the local multiplicity fluctuation study as a signature of critical hadronization in heavy-ion collisions. We report the values of erraticity index for the two versions of the model with default settings and their dependence on the size of the phase space region. Results presented here may serve as a reference sample for the experimental data from heavy ion collisions at these energies.

*email:ragupta@cern.ch

1 Introduction

Dynamics of the initial processes, that is the distributions and the nature of interactions of quarks and gluons, in the heavy ion collisions affect the final distribution of the particles produced [1]. Of the various distributions, multiplicity distributions play fundamental role in extracting first hand information on the underlying particle production mechanism. If QGP is formed at these energies the QGP-hadron phase transition is expected to be accompanied by large local fluctuations in the number of produced particles in the regions of phase space [2]. Thus the study of fluctuations in the multiplicity is an important tool to understand the dynamics of initial processes and consequently the processes of strong interactions, phase transition and also to understand correlations of QGP formation [3].

A comprehensive theoretical model which can explain and give answers to all the complexities of the physics involved at high energy and densities, as is created in the heavy ion collisions, is still not available. A successful model focussed on one aspect of the problem may not say much about the other aspects, but at least should not contradict what is observed. The measures which are studied in the present work rely on the large bin multiplicities. At LHC energies multiplicities are high and it is possible to have detailed study of the local properties in (η, ϕ) space for narrow p_T bins and thus to explore the dynamical properties of the system created in the heavy ion collisions. Thus as an initial attempt to understand the nature of global properties, as manifested in local fluctuations, here we develop and test the methodology and effectiveness of the analysis, analysing simulated events for Pb-Pb collisions at $\sqrt{s_{NN}} = 2.76$ TeV using A Multi-Phase Transport (AMPT) model.

Study of charged particle multiplicity fluctuations is one of the sensitive probes to learn about the properties of the system produced in the heavy ion collisions. Factorial moments are one of the convenient tools for studying fluctuations in the particle production. The concept of factorial moments was first used by A. Bialas and R. Peschanski [4] to explain unexpectedly large local fluctuations in high multiplicity events recorded by the JACEE Collaboratin. Advantage of studying fluctuations using factorial moments is that these filter out statistical fluctuations. The normalised factorial moment F_q is defined as

$$F_q(\delta^d) = \frac{\langle n!/(n-q)! \rangle}{\langle n \rangle^q} \quad (1)$$

where n is the number of particles in a bin of size δ^d in a d -dimensional space of observables and $\langle \dots \rangle$ is either vertical or horizontal averaging. q is the order of the moment and is a positive integer ≥ 2 . Then a power-law behaviour

$$F_q(\delta) \propto \delta^{-\varphi_q} \quad (2)$$

over a range of small δ is referred to as *intermittency*. In terms of the number of bins $M \propto 1/\delta$, Eq. 2 may be written as

$$F_q(M) \propto M^{\varphi_q} \quad (3)$$

where φ_q is the intermittency index, a positive number.

Even if the scaling behaviour in Eq. 2 is not satisfied, to a high degree of accuracy, F_q satisfies the power law behaviour

$$F_q \propto F_2^{\beta_q} \quad (4)$$

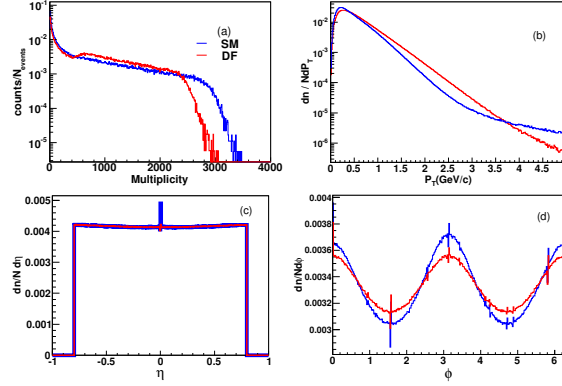


Figure 1: (a) Multiplicity distribution (b) p_T (c) η and (d) ϕ distributions of charged particles generated in Pb-Pb collisions at $\sqrt{s_{NN}} = 2.76$ TeV using the DF and SM AMPT.

This is referred to as F-scaling. In attempts to quantify systems undergoing second order phase transition, in Ginzburg-Landau (GL) theory [5], it is observed that

$$\beta_q = (q-1)^\nu, \quad \nu = 1.304, \quad (5)$$

the scaling exponent, ν , is essentially independent of the details of the GL parameters.

Factorial moments (F_q 's) do not fully account for the fluctuations that the system exhibits. Vertically averaged horizontal moments, can gauge the spatial fluctuations, neglecting the event space fluctuations. On the other hand, horizontally averaged vertical moments lose information about spatial fluctuations and only measure the fluctuations from event-to-event. *Erraticity analysis* introduced in [6], where one finds moments of factorial moment distribution, takes into account the spatial as well as the event space fluctuations. It measures fluctuations of the spatial patterns and quantifies this in terms of an index named as *erraticity index* (μ_q). In a recent work [7], μ_q is observed to be a measure sensitive to the dynamics of the particle production mechanism and hence to the different classes of quark-hadron phase transition.

In erraticity analysis, event factorial moments are studied, defined for an e^{th} event as

$$F_q^e(M) = \frac{f_q^e(M)}{[f_1^e(M)]^q} \quad (6)$$

wherein,

$$f_q^e(M) = \langle n_m(n_m - 1) \dots (n_m - q + 1) \rangle_h \quad (7)$$

where $n_m \geq q$ is the bin multiplicity of the m^{th} bin, and $\langle \dots \rangle_h$ is the average over all bins such that for M^2 cells

$$f_q^e(M) = \frac{1}{M^2} \sum_{m=1}^{M^2} n_m(n_m - 1) \dots (n_m - q + 1) \quad (8)$$

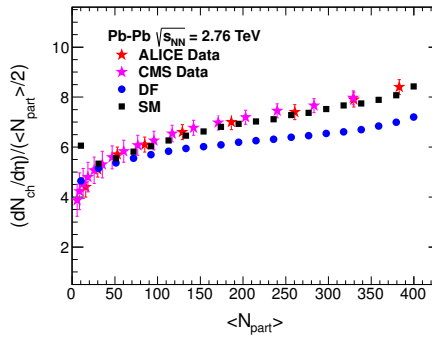


Figure 2: $dN_{ch}/d\eta$ versus N_{part} plot for DF and the SM AMPT, compared with the ALICE and CMS data

Now if $F_q^e(M)$ fluctuates from event-to-event, then the deviation of $F_q^e(M)$ from $\langle F_q^e(M) \rangle_v$ ($\langle \dots \rangle_v$ is for averaging over all events) for each event can be quantified using p^{th} order moments of the normalised q^{th} order factorial (horizontal) moments that can be defined as

$$C_{p,q}(M) = \langle \phi_q^p(M) \rangle_v \quad (9)$$

where p is a positive real number and

$$\phi_q^p(M) = \frac{[F_q^e(M)]^p}{\langle F_q^e(M) \rangle_v^p} \quad (10)$$

To search for M -independent property of $C_{p,q}(M)$ one looks for a power-law behaviour of $C_{p,q}(M)$ in M ,

$$C_{p,q}(M) \propto M^{\psi_q(p)} \quad (11)$$

this is referred to as *erraticity* [6]. If $\psi_q(p)$ is found to have a linear dependence on p , then *erraticity index* μ_q can be defined as

$$\mu_q = \frac{d\psi_q(p)}{dp} \quad (12)$$

in the linear region so that it is independent of both M and p . μ_q is a number that characterizes the fluctuations of spatial patterns from event-to-event. μ_4 is observed [7] to be an effective measure to distinguish different criticality classes, viz., critical, quasicritical, pseudocritical and non-critical, having low value for critical hadronization compared to those having random hadronization. To a good approximation, it is observed [7] that for the model with contraction owing to confinement, μ_4 (critical and quasicritical case) = 1.87 ± 0.84 and for models without contraction μ_4 (pseudocritical and noncritical) = 4.65 ± 0.06 . These model values are suggestive of the significance of erraticity index to characterize dynamical processes.

2 Data Analysed

Charged particles in $|\eta| \leq 0.8$ and full azimuth, generated using two versions of A MultiPhase Transport (AMPT) model [8, 9], in Pb-Pb collisions at $\sqrt{s_{NN}} = 2.76$ TeV are analysed. AMPT model is a hybrid model that includes both initial

p_T window	Default	String Melting
	$\langle N \rangle$	$\langle N \rangle$
$0.2 \leq p_T \leq 0.3$	285.2	434.8
$0.3 \leq p_T \leq 0.4$	279.2	355.5
$0.4 \leq p_T \leq 0.5$	243.7	271.6
$0.6 \leq p_T \leq 0.7$	163.3	155.5
$0.9 \leq p_T \leq 1.0$	80.5	66.1

Table 1: Average Multiplicity of the Simulated Data sets analyzed in different p_T windows

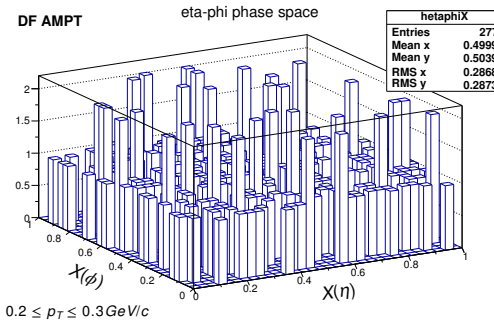


Figure 3: $(X(\eta), X(\phi))$ phase space of an event with $M = 32$ in DF and SM case

partonic and the final hadronic state interactions and transition between these two phases. This model addresses the non-equilibrium many body dynamics. Depending on the way the partons hadronize there are two versions, default (DF) and the string melting (SM). In the DF version partons are recombined with their parent strings when they stop interacting and the resulting strings are converted to hadrons using Lund String Fragmentation model. Whereas in the SM version, a quark coalescence model is used to obtain hadrons from the partons.

We have generated 23424 DF and 19669 SM events with impact parameter, $b \leq 5$, using the model parameters, $a = 2.2$, $b = 0.5$, $\mu = 1.8$ and $\alpha = 0.47$. Multiplicity, p_T , pseudorapidity and ϕ distributions of the simulated events is shown in the Figure 1. Charged particles generated in the $|\eta| \leq 0.8$ and full azimuth having $p_T \leq 1.0$ GeV/c in the small p_T bins of width 0.1 GeV/c are studied for the local multiplicity fluctuations in the spatial patterns. Five p_T bins are considered in the present analysis, as tabulated in the Table 1, along with the average multiplicity of the generated charged particles in the respective p_T bins.

Though AMPT does not contain the dynamics of collective interactions that are responsible for critical behaviour, but it is a good model to test the effectiveness of the methodology of analysis for finding observable signal of quark-hadron phase transition (intermittency analysis) and the quantitative measure of critical behaviour of the system (erraticity analysis) at LHC energies.

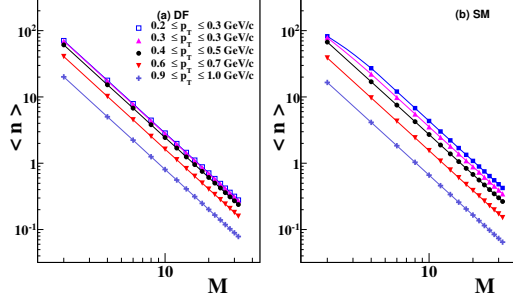


Figure 4: Average bin multiplicity dependence on M for the five p_T bins, in case of DF and the SM AMPT model

3 Analysis and Observations

For an ' e^{th} ' event, the q^{th} order event factorial moment ($F_q^e(M)$) as defined in Eq. (6) are determined so as to obtain a simple characterization of the spatial patterns in two dimensional (η, ϕ) space in narrow p_T windows. However we first obtain flat single particle density distribution using cumulative variable $X(\eta)$ and $X(\phi)$ [10], which are defined as

$$X(y) = \frac{\int_{y_{min}}^y \rho(y) dy}{\int_{y_{min}}^{y_{max}} \rho(y) dy} \quad (13)$$

here y is η or ϕ , y_{min} and y_{max} denote respectively the minimum and maximum values of y interval considered. η and ϕ is mapped to $X(\eta)$ and $X(\phi)$ between 0 and 1 such that $\rho(y)$ is the single particle η or ϕ density. $(X(\eta), X(\phi))$ unit square of an event in a selected p_T window, is binned into a square matrix with M^2 bins where the maximum value that M can take depends on the multiplicity in the Δp_T interval and the order parameter, so that the important part of the M dependence is captured.

To give a visualization of the binning in the (η, ϕ) space in narrow p_T bin, alego plot for an arbitrary event from DF AMPT data, in $0.2 \leq p_T \leq 0.3$ window, with $M = 32$, is shown in Fig. 3.

As value of M and p_T increases, the (η, ϕ) space becomes empty, as is observed from Figure 4 which shows the dependence of the average bin multiplicity ($\langle n \rangle$) on M . Because of the denominator in Eq. (6), a cluster of particles with multiplicity $n \geq q$ in an event would produce a large value for $F_q^e(M)$ for that event. On the other hand, if the particles are evenly distributed, $F_q^e(M)$ would be smaller. Thus the spatial pattern of the event structure should be revealed in the distribution of $F_q^e(M)$ after collecting all events.

Study of the event factorial moment distributions, ($P(F_q)$) reveal that the distributions become wider as M increases and develop long tails at higher q , especially at higher M values. Further the peaks of the distributions shift towards left with increase in M leading to decrease in $\langle F_q^e \rangle$ (referred to as F_q hereafter) with M whereas the upper tails move towards right, at higher q values as M increases. It means that in small bins the average bin multiplicity $\langle n \rangle$ is so small that when there is a spike of particles in one such bin with $n \geq q$, the non-vanishing numerator in

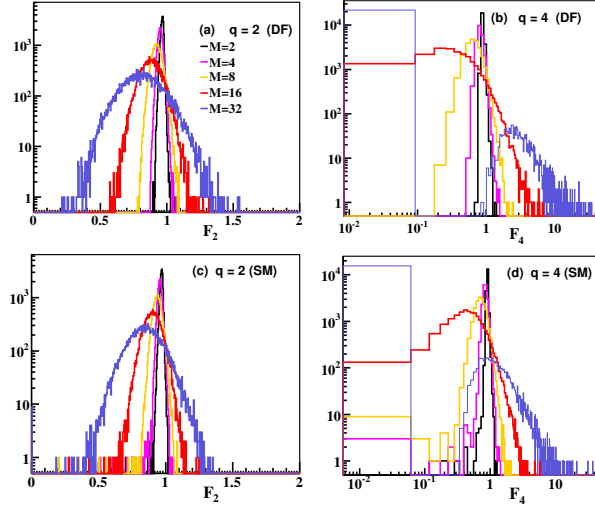


Figure 5: $P(F_q^e)$ distributions for order moment $q = 2$ and $q = 4$ for DF and SM ($0.3 \leq p_T \leq 0.4$). M values in multiples of 2 are shown only.

Eq. (6) results in a large value for $F_q^e(M)$ for that e^{th} event.

Dependence of F_q on M can be studied in log-log plots as shown in Fig. 6 for various p_T cuts. From the plots, it is observed that F_q 's decrease as the bin size decreases or in other words, as M value increases. We observe for both the DF and SM in AMPT that relationship between $F_q(M)$ and M is inverse of that in the Eq. (3); that is

$$F_q^{\text{AMPT}}(M) \propto M^{\varphi_q^-}, \quad \varphi_q^- < 0 \quad (14)$$

Hence, with negative φ_q^- it is found that *the charged particles generated by the default and the string melting version of the AMPT model exhibit negative intermittency*.

Eq. (14) suggests that $F_q^{\text{AMPT}}(M) \rightarrow 0$ at large M and q , implying that in AMPT there are too few rare high-multiplicity spikes anywhere in phase space. Eq. (14) is a quantification of the phenomenon exemplified by Fig. 3 for one event, and is a mathematical characterization after averaging over many events. This same behaviour was observed in [7] for the events belonging to the non-critical class.

We plot F_q versus F_2 in Fig. 7 to check F-scaling. For each set of p_T bins linear fit has been performed to determine the value, β_q , the slope, as exemplified by the straight lines in Fig. 7 (a). The dependence of β_q on $(q - 1)$ is shown in Fig. 8, which exhibits good linearity in the log-log plots. Thus we obtain a scaling exponent, denoted here as ν_- . In Table 2 are given the value of the negative scaling exponent for different p_T windows and for both versions of the AMPT model studied here. Since the scaling that is there in Eq. 3 is different to that we observe here for AMPT data, thus the scaling exponent obtained here cannot be compared with the $\nu = 1.304$ for the second order phase transition, as obtained from the GL theory.

Since large fluctuations result in the high F_q tails of $P(F_q)$, as exemplified in Fig. 5 (b) and (d), it is advantageous to put more weight on the high F_q side in averaging over $P(F_q)$. That is just what the double moment $C_{p,q}(M)$ does. We have determined $C_{p,q}(M)$ for $q = 2, 3, 4, 5$ and $p = 1.0, 1.25, 1.5, 1.75$ and 2.0 .

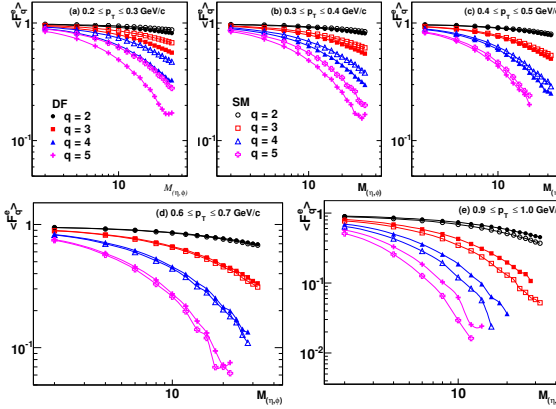


Figure 6: M Dependence of F_q , for DF as well as SM.

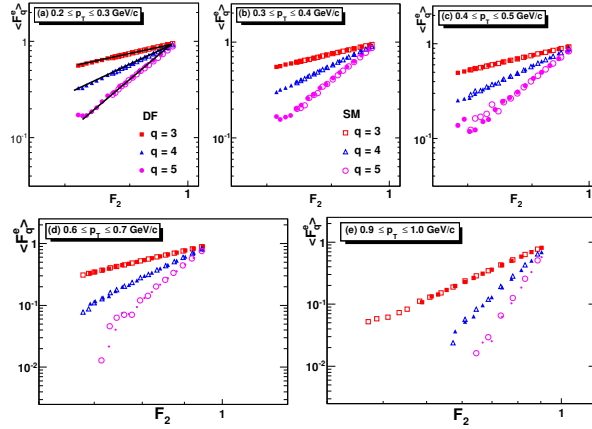
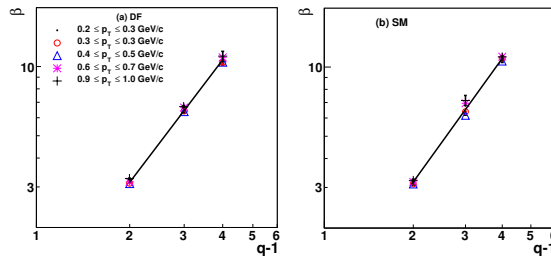


Figure 7: F-Scaling for DF as well as SM mode of AMPT

The number of bins, M , takes on values from 2 to the maximum value possible while having reasonable $\langle n_m \rangle$ such that $F_q \neq 0$. To check whether $C_{p,q}(M)$ follows the scaling behaviour with M , $C_{p,q}$ is plotted against M . Fig. 9 (a) to (d) shows respectively, for $q = 2, 3, 4$ and 5 , the $C_{p,q}$ versus M plot in the log-log scale for the window $0.6 \leq p_T \leq 0.7$ GeV/c, and for various values of p between 1 and 2. As expected for all values of q , for $p = 1.0$, the $C_{p,q} = 1$. For $p > 1.0$, $C_{p,q}$ increases with M and q values. Similar calculations are also done for the other p_T windows. In the high M region linear fits are performed for each q and p value so as to determine $\psi_q(p)$. We see in Fig. 10 that for $0.6 \leq p_T \leq 0.7$ $\psi_q(p)$ depends on p linearly for each q . Thus the erraticity indices defined in Eq. (12) are determined. Similar plots are obtained for the other p_T windows also and the values of μ_q are given in Table 3. It can be seen from the table that as p_T value increases, the erraticity indices increase for both versions of the AMPT model.

Comparing the μ_q values for the DF and SM data within the same window and for the same values of q , it is observed that μ_q has higher values for the DF version in comparison to SM for the p_T windows below 0.6 GeV/c. That phenomenon


 Figure 8: β_q versus $(q - 1)$ plot for determination of the scaling exponents.

p_T	ν_- (Default)	ν_- (String Melting)
$0.2 \leq p_T \leq 0.3$	1.738 ± 0.008	1.753 ± 0.004
$0.3 \leq p_T \leq 0.4$	1.774 ± 0.007	1.793 ± 0.005
$0.4 \leq p_T \leq 0.5$	1.758 ± 0.006	1.755 ± 0.006
$0.6 \leq p_T \leq 0.7$	1.824 ± 0.008	1.869 ± 0.016
$0.9 \leq p_T \leq 1.0$	1.778 ± 0.013	1.781 ± 0.011

Table 2: Scaling exponents for negative intermittency in the Default and String Melting versions of the AMPT Model

is related to the average multiplicities of the two versions reversing their relative magnitudes at higher p_T . However it is to be noted from Fig. 10 that the dependence of $\psi_q(p)$ on p is better distinguishable for the two versions of the AMPT for only $q = 4$. Coincidentally, as observed in [7], μ_4 seems to be a good measure to compare the erraticity indices of the different systems and data sets at these energies.

We observe that the values of μ_4^{DF} and μ_4^{SM} for all p_T windows are larger than those obtained for the critical data set in [7], on the same side as the non-critical case. We have found φ^- to be negative because $P(F_q)$ broadens, as M increases, with $\langle F_q e \rangle$ shifting to the lower region of F_q^e , thus resulting in negative intermittency. We did notice that the upper tails move to the right, suggesting the presence of some degree of clustering. To emphasize that part of $P(F_q)$ we have taken higher p -power moments of $\phi_q(M)$, which suppress the lower side of F_q while boosting the upper side. The scaling properties of $C_{p,q}(M)$ therefore deemphasize what leads to negative intermittency. Thus the erraticity indices μ_q reveal a different aspect of the fluctuation patterns than the scaling indices ν^- . Our study here has revealed interesting properties of scale-invariant fluctuations that should be compared to the real data.

4 Summary

Fluctuations in the spatial patterns of charged particles and their event-by-event fluctuations, as are present in the events generated using the default and string melting version of A MultiPhase Transport (AMPT) model are studied. This is a first attempt to study intermittency and erraticity at such high energies. It is observed that as the bin size decreases, the factorial moments decrease. This behaviour is in contrast to usual properties of intermittency observed at lower energies indicating

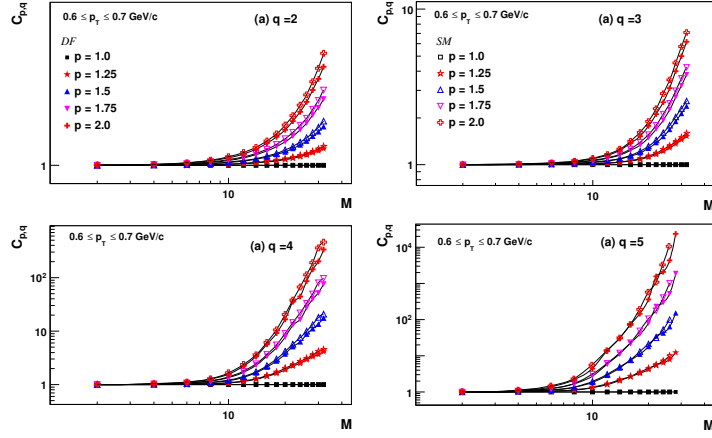


Figure 9: M dependence of $C_{p,q}$ for the p_T window $0.6 \leq p_T \leq 0.7 \text{ GeV}/c$ in case of DF and SM versions of the AMPT model

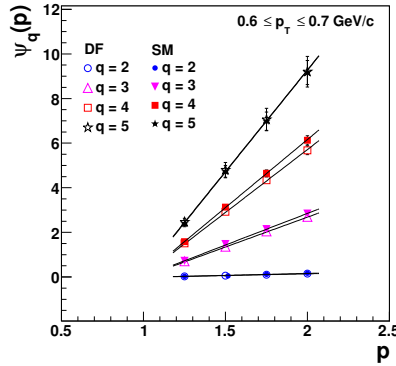


Figure 10: The ψ_q dependence on the p for DF and SM AMPT in the $0.6 \leq p_T \leq 0.7 \text{ GeV}/c$ window.

that events with localization of even moderate multiplicities in the small bins, at low p_T are not present in the AMPT. Further the erraticity analysis of the model shows that the systems generated in it is not near criticality. The μ_q values determined here give the quantification of the event-by-event fluctuations in the spatial patterns of the charged particles in the midrapidity region, which can be used effectively to compare with other models. More importantly comparison of the values with that from the LHC would help to get a better understanding of the particle production mechanism at high energies.

References

- [1] S. Gavin and George Moschelli, Phys. Rev. C **85**, 014905 (2012).
- [2] M.I. Adamovich *et al.*, Phys. Lett. B, **201**, 3, 397 (1988).

p_T	AMPT (Default)	AMPT (String Melting)
	μ_2	μ_2
$0.2 \leq p_T \leq 0.3$	0.043 ± 0.002	0.016 ± 0.001
$0.3 \leq p_T \leq 0.4$	0.045 ± 0.002	0.027 ± 0.001
$0.4 \leq p_T \leq 0.5$	0.062 ± 0.003	0.048 ± 0.002
$0.6 \leq p_T \leq 0.7$	0.154 ± 0.008	0.174 ± 0.011
$0.9 \leq p_T \leq 1.0$	0.739 ± 0.043	1.014 ± 0.064
	μ_3	μ_3
$0.2 \leq p_T \leq 0.3$	0.901 ± 0.081	0.328 ± 0.025
$0.3 \leq p_T \leq 0.4$	0.904 ± 0.081	0.531 ± 0.043
$0.4 \leq p_T \leq 0.5$	1.304 ± 0.118	1.019 ± 0.077
$0.6 \leq p_T \leq 0.7$	2.678 ± 0.155	2.832 ± 0.137
$0.9 \leq p_T \leq 1.0$	4.502 ± 0.147	4.960 ± 0.305
	μ_4	μ_4
$0.2 \leq p_T \leq 0.3$	4.325 ± 0.243	2.481 ± 0.183
$0.3 \leq p_T \leq 0.4$	4.532 ± 0.234	3.385 ± 0.235
$0.4 \leq p_T \leq 0.5$	5.478 ± 0.258	3.935 ± 0.021
$0.6 \leq p_T \leq 0.7$	5.640 ± 0.203	6.101 ± 0.214
$0.9 \leq p_T \leq 1.0$	7.484 ± 0.361	7.359 ± 0.305
	μ_5	μ_5
$0.2 \leq p_T \leq 0.3$	6.202 ± 0.302	5.143 ± 0.022
$0.3 \leq p_T \leq 0.4$	6.150 ± 0.175	5.745 ± 0.312
$0.4 \leq p_T \leq 0.5$	7.396 ± 0.437	6.159 ± 0.280
$0.6 \leq p_T \leq 0.7$	9.107 ± 0.693	8.360 ± 0.533
$0.9 \leq p_T \leq 1.0$	8.643 ± 0.537	7.655 ± 0.358

- [3] L. VanHove, Z. Phys. C **27** (1985), M. Gyulassy *et al.*, Nucl. Phys. B **237**, 477-501 (1984).
- [4] A. Bialas and R. Peschanski, Nucl. Phys B **273** 703 (1986); B **308**, 867 (1988).
- [5] R.C. Hwa and M.T. Nazirov, Phys. Rev. Lett. **69**, 741 (1992).
- [6] Z. Cao, R. Hwa, Phys. Rev. Lett. **75**, 1268 (1995), Phys. Rev. D **53**, 6608 (1996); Phys. Rev. D **54**, 6674 (1996).
- [7] R.C. Hwa and C.B. Yang, Phys. Rev. C **85**, 044914 (2012).
- [8] B. Zhang, C.M. Ko, B.A. Li and Z.W. Lin, Phys. Rev. C **61**, 067901 (2000).
- [9] Z.W. Lin, C.M. Ko, B.A. Li, B. Zhang and S. Pal, Phys. Rev. C **72**, 064901 (2005).
- [10] W. Ochs, Z Phys. C **50**, 339 (1991).